energy&fuels

Article

pubs.acs.org/EF

# High-Pressure Oxy-Firing (HiPrOx) of Fuels with Water for the Purpose of Direct Contact Steam Generation

Paul E. C. Cairns,*[,†] Bruce R. Clements,[†] Robin Hughes,[†] Ted Herage,[†] Ligang Zheng,[†] Arturo Macchi,[‡] and Edward J. Anthony[§]

[†]Natural Resources Canada, CanmetENERGY, 1 Haanel Dr., Ottawa, Ontario, Canada, K1A 1M1

[‡]Faculty of Chemical and Biological Engineering, University of Ottawa, 161 Louis Pasteur St., Ottawa, Ontario, Canada, K1N 6N5

[§]School of Applied Sciences, Cranfield University, College Rd., Cranfield, Bedford MK43 0AL, United Kingdom

Supporting Information

**ABSTRACT:** High-pressure oxy-fired direct contact steam generation (HiPrOx/DCSG) can be achieved by the oxy-combustion of fuels in the presence of water. This process is capable of producing flue gas streams containing approximately 90% steam with a balance of primarily $CO_2$. The product flue gas is suitable for processes where the purity of the steam is less important, such as the steam-assisted gravity drainage process used for *in situ* production of bitumen within the Canadian oil sands. This study had three primary objectives: (1) To show that high-moisture HiPrOx/DCSG can be achieved with hydrocarbon fuels. For this purpose, *n*-butanol was used because of its high volatility and ease of handling. (2) To see if this technology could be applied to fuels with lower volatilities. This was studied by attempting to combust a graphite−water slurry as well as mixtures of graphite−water slurry and butanol. (3) To determine the effects of different fuel mixtures, oxygen-to-fuel ratios, and water inputs on process stability and $H_2O$ partial pressure in the product gas. This paper describes pilot-scale combustion testing and process modeling of *n*-butanol, graphite−water slurry, and their mixtures in an atmosphere consisting of oxygen and water at a pressure of 1.5 MPa(g). Graphite/butanol mixtures were selected because certain combinations could represent the range of fixed carbon/volatiles ratios of waste fuels and indicate whether low-volatile fuels will ignite in the high-water moderator environment. Over the butanol test periods, a steam content of around 90 mol % at saturation was achievable; the $O_2$ in the combustion products was between 0.08 and 3.57 mol % (wet) with an average of 1.13 mol % (wet). The CO emissions were low (<25 ppmv wet, 3% $O_2$) in the combustor. The CO levels indicated that high fuel conversion was achieved with low excess $O_2$ content in the combustion products. The testing also indicated that operation with extremely low $O_2$ is possible for specific fuels, which will minimize downstream corrosion issues and reduce the energy consumption and costs associated with oxygen production requirements. Low CO emissions (<25 ppmv wet, 3% $O_2$) and relatively good process stability were experienced for the butanol/graphite−water slurry mixtures containing ~40% butanol. CO emissions increased and process stability decreased as the graphite content in the fuel mixture was increased. Unassisted combustion of the graphite−water slurry was achieved for a period of 20 minutes until operational problems were encountered, due to burner plugging by the slurry, requiring that the burner be shut off. It was found that the maximum attainable $H_2O$ content in the product gas increased with increasing hydrogen-to-carbon ratio in the fuel. $H_2O$ content was around 80 mol % with 100% graphite−water slurry, 81 mol % with a 25% butanol in graphite−water slurry mixture, and around 86.5% in a 40% butanol in graphite−water slurry mixture. It was also found that the fuel H/C ratio, excess $O_2$, heat loss, $O_2$ purity, and fuel volatility are important parameters when considering a DCSG system because they directly affect the process performance and quality of the desired product.

## 1. INTRODUCTION

Canada has the third largest oil reserves in the world. Of Canada's 173 billion barrels of oil reserves, 170 billion barrels are located in Alberta, of which 168 billion barrels can be derived from bitumen.[1] Oil sands bitumen is a resource that has been developed for decades but is now gaining increased global attention as conventional supplies continue to be depleted.[1] In 2011, thermal *in situ* operations such as steam-assisted gravity drainage (SAGD) accounted for 49% of the bitumen production in Alberta.[2] While *in situ* extraction methods are less invasive than mining and have less local environmental impacts, SAGD results in more greenhouse gas (GHG) emissions per barrel[3] and requires large amounts of water that must be treated and recycled, with around a 10−20% make-up water requirement.[2] CanmetENERGY is developing a new steam generation technology known as the high-pressure oxy-fired direct contact steam generator (HiPrOx/DCSG, or simply DCSG) that will reduce water requirements and simultaneously sequester GHGs while extracting heavy oil. The HiPrOx/DCSG technology is described in the CanmetENERGY patent entitled *"High pressure direct contact oxy-fired steam generator"* and is intended to replace the once through steam generators (OTSGs) and drum boilers that are currently used for SAGD.[4] The ultimate goal of CanmetENERGY's HiPrOx/DCSG program is to combust natural gas, low quality liquid fuels, and/or waste fuels such as petroleum coke at high pressure (9.0 MPa) in the DCSG mode.

**Received:** December 8, 2014
**Revised:** April 10, 2015
**Published:** July 7, 2015





DOI: 10.1021/ef502754h
*Energy Fuels* 2015, 29, 4522−4533

Ideally, the moderating water would be wastewater containing high solids and hydrocarbon contamination such as tailings water produced from mining and upgrading, SAGD produced oily water (POW), and/or SAGD produced water (PW).

For HiPrOx/DCSG, a fuel is combusted with pure oxygen at high pressure using water, which may be contaminated with hydrocarbons and solids, as a moderator to create the final product, a flue gas stream consisting mainly of steam with a minor portion of $CO_2$. The product can be injected into an underground bitumen reservoir where the heat of the product is transferred to the bitumen to reduce its viscosity, allowing it to be pumped to the surface via a production well. It is important that the product contain a high concentration of $H_2O$ because its latent heat plays the largest role in heating the bitumen. A modeling study performed by Gates et al.[5] predicted that approximately 80% of the $CO_2$ that is injected into the reservoir is sequestered, making this technology a competitive CCS technology for the oil sands. Since the combustion products of this technology are all converted to the useable product that is injected into the well, the thermal efficiency of this device will likely be above 95%. An energy and material balance study of the DCSG technology applied to a SAGD process at a pressure of 10 MPa was performed by CanmetENERGY.[6] It was found that the energy intensity ($MW_{th}$ in/$MW_{th}$ out) decreased by 3.6−7.6% compared to an OTSG system without CCS and by 8.2−12.0% compared to an OTSG system with CCS.[6] Although the air separation unit increases electrical utility requirements (from 45 $MW_{th}$ equivalent for the base case to 143.4 $MW_{th}$ equivalent for the DCSG case, based on 33% electrical conversion efficiency), the reduction in fuel heat input is greater (from 483 $MW_{th}$ for the base case to 374 $MW_{th}$), resulting in an overall reduction in energy intensity.[6] The large reduction in fuel requirements results from the use of the combustion products directly in the process product. Therefore, any $H_2O$ produced as a result of fuel conversion is sent directly down well along with the steam, as opposed to being sent up the flue stack for the conventional boiler case. Thus, less fuel is required to produce the same amount of steam because the product steam comes from the hydrogen in the fuel as well as the conventional steam produced via its thermal energy.

Direct-contact air-fired steam generators and downhole steam generation have been in existence for a number of years. Several demonstrations have been carried out with relatively positive results.[7−9] Many of these direct contact steam generation configurations were oriented toward the use of natural gas as opposed to solid fuels.[10] Work on the combustion and gasification of fuels is mostly focused on solid fuels utilization in power generation systems, with the exception of natural gas combined cycle (NGCC) and oil residue gasification. The main flue gas constituents in air-fired combustion systems are typically $N_2$, $H_2O$, and $CO_2$ with some CO.[11−20] The main flue gas constituents for the gasification systems are typically CO and $H_2$, with some $H_2O$ and $CO_2$.[11−20] In contrast, this study is targeted toward flue gases where $H_2O$ is the major constituent, with concentrations of steam closer to 90%. Although our fuel conversion approach is different, previous combustion and gasification work provides a technology base to aid in the commercialization of the DCSG process with gaseous, liquid, and solid fuels.

Steam addition was studied for ambient pressure oxy-firing of semianthracite and high-volatile bituminous coals by Riaza et al.[21] It was shown that the ignition temperature was increased and burnout was reduced for a reactant oxygen concentration of 21%; however, as the oxygen concentration was increased to 30% and 35%, the ignition temperature decreased and burnout improved. They postulated that the results may be related to enhancements in thermal radiation or endothermic radical formation (O·, OH·, H·, etc.). Seepana and Jayanti[22] performed a theoretical study of steam-moderated oxy-fuel combustion of methane. In their study, flame structure analysis using a 325-step reaction mechanism was performed. They determined that higher oxygen content in the oxidant stream was required in order to obtain the same flame structure when moderating with steam compared to $CO_2$. This resulted in a much higher mass fraction of oxygen in the flue gas. For a DCSG process, the need for higher $O_2$ concentrations in the flue gas may prove to be a disadvantage because higher concentrations of oxygen in the flue gas make corrosion problems a greater issue[23] and the generation of oxygen is energy intensive and expensive. Therefore, reducing the oxygen requirement is beneficial for economic and efficiency reasons. Although the aforementioned studies suggest that steam addition to oxy-fired flames appears unfavorable,[21,22] those studies were performed at ambient pressure. Pressurized DCSG may prove to be more favorable due to increased fuel throughput, and enhancements in intensity of reaction.[20] These benefits may result in a lower $O_2$ requirement compared to ambient systems.

One of the fuels of interest for use with DCSG is petroleum coke. Petroleum coke is a low-volatile fuel which contains high amounts of sulfur that leads to the formation of sulfuric acid. One of the objectives of these tests was to determine whether fuels with very little volatile matter and relatively inert char can be used within the HiPrOx/DCSG environment. For this testing, graphite and butanol were selected due to the absence of sulfur, which alleviated concerns over corrosion caused by sulfuric acid for which the pilot-scale reactor was susceptible to at the time.

Graphite is chemically unreactive and has attractive mechanical and thermophysical properties. It is thus typically used for high-temperature heat shielding, structural material for atmospheric re-entry, gas turbine blades, scram-jet combustors, etc.[24] As a result, combustion studies involving graphite are typically done in extreme environments. For example, combustion of graphite in high-pressure and high-temperature $CO_2$ and $H_2O$ environments was studied by Culbertson and Brezinsky[25] to determine whether the postcombustion gases were reacting with rocket nozzles and causing erosion. They performed shock-tube testing in pressures ranging from 21.18 to 36.78 MPa and temperatures ranging from 1275 to 2420 °C in pure $CO_2$ and pure steam. They found that the $CO_2$ and steam were indeed reacting with the graphite and also found that both reactions had the same rate coefficient at those conditions. Makino et al.[24] studied the combustion rate of graphite rods in water vapor flow with the purpose of minimizing hazardous disasters caused by the chemical reaction between overheated graphite moderators and water vapor in nuclear reactors. Their study was performed with pure steam at approximately 0.8 MPa and around 1325 °C to determine the reactivity in steam compared to the reactivity in $O_2$ and $CO_2$. They found that $H_2O$ oxidized graphite at a rate lower than $O_2$ and it oxidized graphite at about twice the rate of $CO_2$.

Graphite is much more difficult to burn than petroleum coke due to its lower volatility, higher activation energy, highly stable molecular structure, and lack of porosity. A char combustion reactivity study was performed by Lang and Hurt,[26] in which they produced various solid fuel chars in nitrogen at 700 °C and performed nonisothermal thermogravimetric analyzer tests at a heating rate of 7 °C/min to 950 °C to compare their reactivities. Their study found that the standard reactivity at 500 °C was 14



DOI: 10.1021/ef502754h
Energy Fuels 2015, 29, 4522−4533

**Table 1. Chemical Analysis of *n*-Butanol**

| parameter | value |
|---|---|
| specific gravity @ 25 °C | 0.808 |
| composition | |
| *n*-butanol (wt %) | 99.9 |
| water (wt %) | 0.01 |
| higher heating value [HHV] (MJ/kg) | 33.1 |
| hydrogen-to-carbon ratio [H/C ratio] (by weight) | 0.2154 |

times greater for the delayed petroleum coke char than a graphite powder char. Although the low heating rates and characteristic temperatures of the Lang and Hurt study do not fully represent the high heating rates and temperatures observed in typical combustion applications, their results help illustrate the difficulty of burning graphite compared to the characteristically difficult to burn petroleum coke.

For maximum SAGD process efficiency, it is important to maximize the partial pressure of $H_2O$ in the product gas using the least amount of fuel possible. Lower partial pressure will reduce the saturation temperature, and thus, SAGD reservoir temperature, which reduces bitumen production.[6] This study had three primary objectives: (1) To prove that high moisture HiPrOx/DCSG can be achieved with hydrocarbon fuels. For this purpose, *n*-butanol was used because of its high volatility and ease of handling. (2) To determine if this technology could be applied to fuels with lower volatilities. This was studied by attempting to combust a graphite−water slurry, as well as mixtures of graphite−water slurry and butanol. (3) To determine the effects of different fuel mixtures, oxygen-to-fuel ratios, and water inputs on process stability and $H_2O$ partial pressure in the product gas. As a first step to proving the feasibility of this technology, combustion of *n*-butanol, graphite−water slurry, and mixtures thereof was performed in a HiPrOx/DCSG system at 1.5 MPa(g) pressure with co-injection of municipal water. Process stability was measured by monitoring the fluctuations in reactor pressure and temperature. The CO concentration was measured for periods in which the oxygen/fuel stoichiometric ratio was greater than 1 to help indicate the conversion efficiency of the process. Process simulations of the experimental data were performed to examine the effects of different fuel mixtures, oxygen-to-fuel ratios, and water inputs on $H_2O$ partial pressure in the product gas. This was done to determine which parameters maximize the $H_2O$ partial pressure without greatly affecting process stability. These data will aid in the future design of DCSG processes to provide maximum efficiency and reservoir temperature.

## 2. METHODS

This study consisted of two distinct methods: pilot-scale testing and process modeling. The first method was a pilot-scale demonstration of the feasibility of this technology. The pilot-scale demonstration was performed via the combustion of *n*-butanol ($C_4H_9OH$), graphite−water slurry, and mixtures thereof, with 99.5 mol % pure oxygen and clean city water as a moderator at an operating pressure of 1.5 MPa(g). The bottoms and fly ash were collected in liquid and gas bag filters to measure the carbon losses. The excess oxygen and fuel volatile content were varied while the reactor pressure and temperature fluctuations and dry product gas concentration ($O_2$, $CO_2$, CO) were measured. These parameters were varied to determine their effect on process stability and overall combustion performance. Process stability was measured by taking the sample standard deviation of temperature and pressure over the given test period. The sample standard deviation was calculated using eq 1 below

$$\text{Sample Standard Deviation} = \sqrt{\sum \frac{(x - \bar{x})^2}{(n - 1)}} \quad (1)$$

where "$x$" is each value in the set, "$\bar{x}$" is the average (statistical mean) of the set of values, and "$n$" is the number of values.

The second method consisted of performing process simulations using AspenTech HYSYS. Process simulations of the pilot-scale test conditions were performed to determine the effect of excess oxygen, heat loss, and fuel mixture on the maximum theoretically attainable $H_2O$ content and saturated product gas composition. Further process simulations were performed in which different variables were isolated (heat loss, excess oxygen, fuel hydrogen-to-carbon ratio, etc.). These simulations were used to provide insight into how these variables affect the overall product gas composition and maximize the $H_2O$ concentration (partial pressure) in the product gas.

**2.1. Fuel Description.** Although *n*-butanol is not a practical fuel for an industrial application, it is a suitable research fuel when entering into a trial for proof-of-concept due to its volatility and well-defined chemical and physical properties and the simplicity of using liquid fuel delivery

**Table 2. Butanol/Graphite (BG) Mixture and Graphite (G) Analyses**

| parameter | BG1 | BG2 | BG3 | BG4 | G1 and G2 |
|---|---|---|---|---|---|
| fuel mixture | | | | | |
| butanol (wt %) | 41.6 | 40.8 | 40.9 | 26.3 | 0.0 |
| graphite (wt %) | 58.4 | 59.2 | 59.1 | 73.7 | 100.0 |
| sum (wt %) | 100.0 | 100.0 | 100.0 | 100.0 | 100.0 |
| ultimate analysis (dry) | | | | | |
| C (wt %) | 85.4 | 85.7 | 85.6 | 90.8 | 99.4 |
| H (wt %) | 5.6 | 5.5 | 5.5 | 3.6 | 0 |
| N (wt %) | 0.0 | 0.0 | 0.0 | 0.0 | 0 |
| O (wt %) | 9.0 | 8.8 | 8.8 | 5.7 | 0.6 |
| S (wt %) | 0.0 | 0.0 | 0.0 | 0.0 | 0 |
| sum (wt %) | 100.0 | 100.0 | 100.0 | 100.0 | 100 |
| proximate analysis | | | | | |
| moisture (wt %) | 0.0 | 0.0 | 0.0 | 0.0 | 0 |
| fixed carbon (wt %) | 58.4 | 59.2 | 59.1 | 73.7 | 99.46 |
| volatiles (wt %) | 41.6 | 40.8 | 40.9 | 26.3 | 0.54 |
| ash (wt %) | 0.0 | 0.0 | 0.0 | 0.0 | 0 |
| calorific analysis (dry) | | | | | |
| HHV (MJ/kg) | 33.7 | 33.7 | 33.7 | 33.4 | 32.77 |
| H/C ratio (by weight) | 0.0659 | 0.0643 | 0.0645 | 0.0391 | 0 |



DOI: 10.1021/ef502754h
*Energy Fuels* 2015, 29, 4522−4533

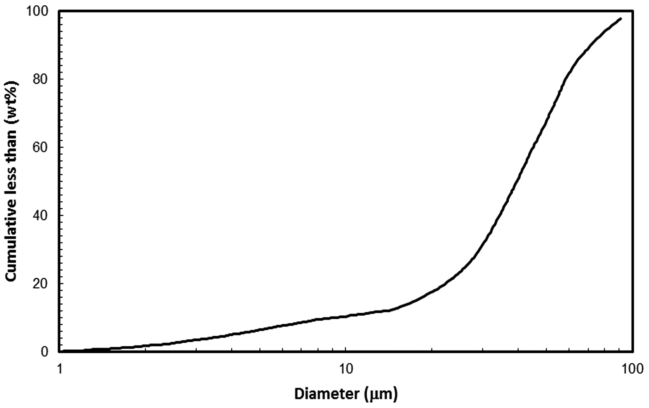


**Figure 1.** Graphite particle size distribution.

**Table 3. Butanol Test Condition Summary**

| description | B1 | B2 | B3 | B4 |
|---|---|---|---|---|
| butanol flow (kg/h) | 11.5 | 15.2 | 15.2 | 15.2 |
| total heat input ($kW_{th}$) | 105.7 | 139.6 | 139.6 | 139.6 |
| oxygen flow (kg/h) | 33.5 | 40.4 | 39.8 | 39.6 |
| molar oxygen-to-fuel stoichiometric ratio | 1.125 | 1.027 | 1.012 | 1.005 |
| burner moderator flow (kg/h) | 32.5 | 50.0 | 50.0 | 50.0 |
| burner nitrogen flow (kg/h) | 0.0 | 0.0 | 0.0 | 2.1 |
| adiabatic flame temperature (°C)[a] | 1939 | 1802 | 1807 | 1809 |

[a]Calculated using AspenTech HYSYS.

compared to compressed gases (e.g., high-pressure natural gas). Typically, *n*-butanol is used as a solvent, but may be used as a fuel. The analysis of the butanol used in these tests is given in Table 1. Various graphite/butanol mixtures were also tested in order to represent the range of proximate analyses of coal and other waste fuels. The fuel analyses for the graphite and the butanol/graphite mixtures are provided in Table 2. The graphite−water slurry was fed through a slurry line where it was combined with the butanol via a tee. The slurry was made by filling a slurry mixing tank supported by load cells, with water. The graphite powder was added based on a target solids loading of 40 wt %. The slurry was allowed to mix overnight via a mixer and a circulating pump. The morning of the test, the viscosity and solids loading were checked and adjusted by adding more water or graphite to reach the targeted solids loading of 40 wt % and viscosity of 760 cP. The typical graphite particle size distribution is given in Figure 1.[27] The size distribution was performed by the manufacturer over many samples using Laser Malvern analysis. The characteristic size of the graphite particles was 60% less than 45 $\mu$m (325 Tyler mesh).

**2.2. Test Matrix.** The pilot facility was operated at four butanol conditions (B1−B4), as summarized in Table 3, four mixtures of butanol and graphite conditions (BG1−BG4), and two graphite conditions (G1 and G2), as summarized in Table 4.

The purpose of condition B1 was to establish that a stable and controllable flame could be achieved while co-injecting liquid water with the fuel. The purpose of conditions B2 and B3 was to evaluate the quality of combustion with little excess oxygen. The purpose of B4 was to gain insight into the effect that noncondensable gases have on the product gas $H_2O$ concentration. This was examined by adding small amounts of $N_2$.

The purpose of BG1 and BG2 was to establish a stable and controllable flame while injecting *n*-butanol, graphite−water slurry, municipal water, and oxygen. The goal of BG3 was to examine the effect of a lower excess $O_2$ on the CO emissions and flame stability. Test condition BG4 examined what effect a lower *n*-butanol fraction in the fuel mixture would have on emissions and stability. After tests BG1−BG4 were carried out, the butanol was completely turned off (G1 to G2)

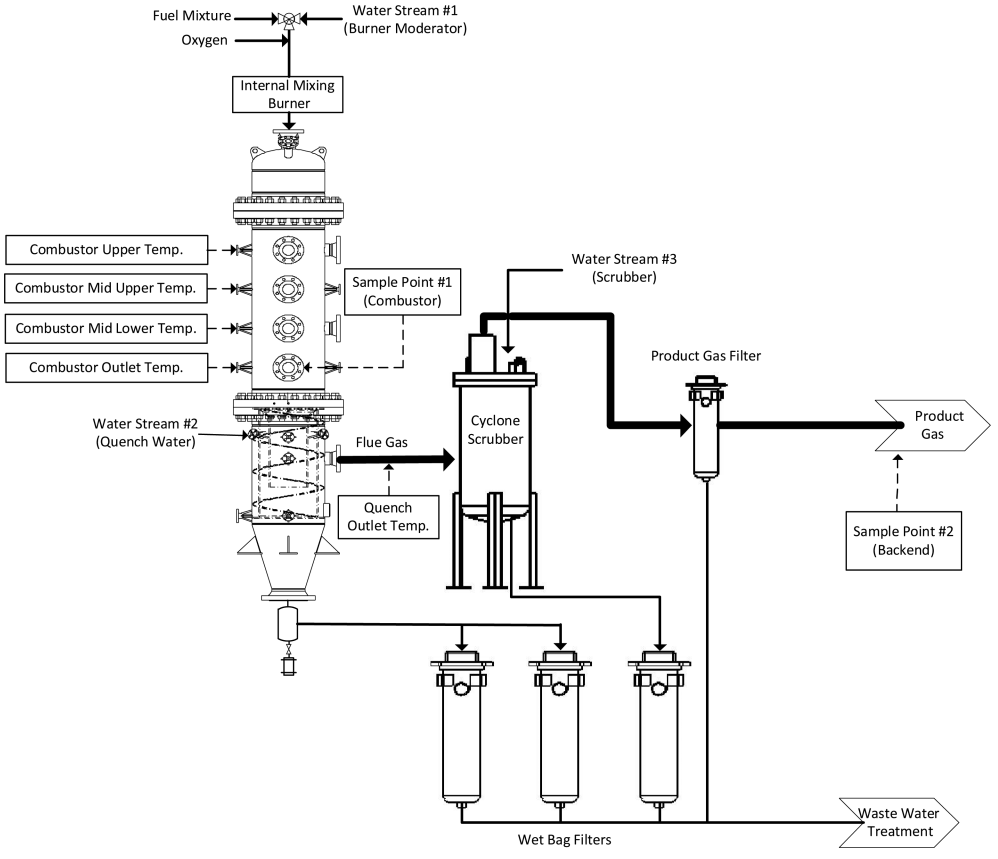


**Figure 2.** 1500 kPa(g) pilot-scale reactor.



DOI: 10.1021/ef502754h
*Energy Fuels* 2015, 29, 4522−4533

**Table 4. Graphite and Mixture Test Conditions Summary**

| description | BG1 | BG2 | BG3 | BG4 | G1 | G2 |
|---|---|---|---|---|---|---|
| butanol flow (kg/h) | 8.0 | 8.0 | 8.0 | 4.1 | 0.0 | 0.0 |
| slurry flow (kg/h) | 28.1 | 28.9 | 28.8 | 28.5 | 30.5−36.0 | 40.0−43.0 |
| slurry solids loading (wt %) | 40.0 | 40.0 | 40.0 | 40.0 | 40.0 | 40.0 |
| average heat input ($kW_{th}$) | 175.7 | 178.5 | 178.1 | 140.9 | 126.1 | 150.8 |
| butanol heat input (%) | 41.8 | 41.0 | 41.1 | 26.4 | 0.0 | 0.0 |
| graphite heat input (%) | 58.2 | 59.0 | 58.9 | 73.6 | 100.0 | 100.0 |
| oxygen flow (kg/h) | 52.1 | 52.8 | 51.5 | 51.3 | 50.3 | 49.6 |
| molar oxygen-to-fuel stoichiometric ratio | 1.051 | 1.048 | 1.024 | 1.273 | 1.31−1.547 | 1.082−1.163 |
| burner moderator flow (kg/h) | 42.0 | 41.0 | 41.1 | 20.7 | 3.9 | 21.0 |
| total water to burner (kg/h) | 58.8 | 58.3 | 58.4 | 37.7 | 22.2−25.5 | 45.0−46.8 |
| adiabatic flame temperature (°C)[a] | 1959 | 1989 | 1994 | 2134 | 2293−2422 | 2066−2136 |

[a]Calculated using AspenTech HYSYS.

**Table 5. Analyzer Accuracy and Characteristic Response Times**

| | analyzer model | | |
|---|---|---|---|
| property | MPA-510 | VIA-510 | VIA-510 |
| species | $O_2$ | $CO_2$ | CO |
| measuring range | 0−25 vol % | 0−100 vol % | 0−2500 ppmv |
| reproducibility over majority of range (±) | 0.125 vol % | 0.5 vol % | 12.5 ppmv |
| bottom of range | <5 vol % | <5 vol % | <100 ppmv |
| reproducibility at bottom of range (±) | 0.25 vol % | 1 vol % | 25 ppmv |
| response time (s) | 30 | 30 | 30 |

and unassisted combustion of graphite−water slurry was initiated. The primary goal of these test conditions was to see if a flame could be self-sustained in a stable fashion.

**2.3. Equipment Description.** The experimental work was performed at 1.5 MPa(g) pressure in the pilot-scale slagging reactor (Figure 2) at CanmetENERGY. The refractory-lined reactor had an inner diameter of 0.25 m and a length of 2.135 m.

The fuel, water, and oxygen were injected into the reactor through an externally cooled gas-swirl atomizer, shown in Figure 3, with an impinging plate and pintle to provide a hollow cone spray. An internal mixing gas-swirl atomizer was selected for these experiments because it is a robust mechanical atomizer capable of finely atomizing the moderator water regardless of the various oxygen and fuel flow rates that were experienced for different test conditions. Other nozzles, such as externally atomized nozzles, are more dependent on feed flows and momentums to obtain the desired atomization. Although this injector design may be susceptible to erosive wear from use with slurried solid fuels over a longer period of time, the run lengths in this work did not result in substantial wear to the pintle. Future work, in which changing the feed flow rates is not a part of the scope, will investigate the use of different types of nozzles where the nozzle can be more thoroughly designed to match the given momentums.

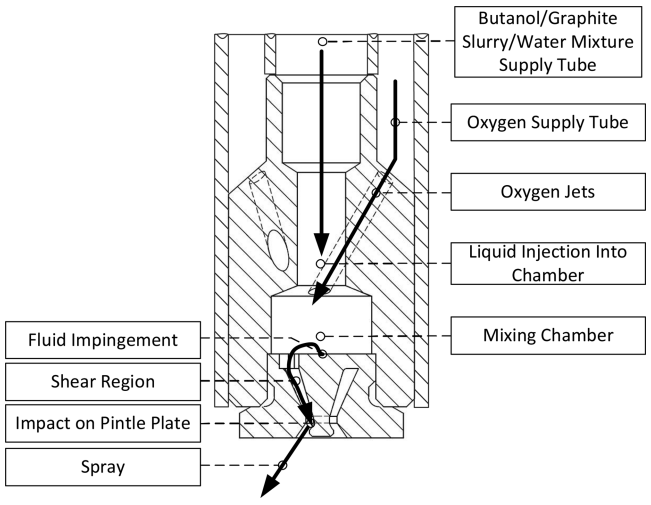


**Figure 3.** Gas-swirl atomizer used for atomizing butanol/graphite slurry/water mixture with oxygen.

For the butanol tests, the *n*-butanol and burner water (Figure 2, water stream #1) were mixed and sent into the mixing chamber via the supply tube (Figure 3). For the butanol/graphite tests, graphite−water slurry, *n*-butanol, and burner water were mixed in the same location.

Oxygen (99.5 mol %) was introduced into the mixing chamber through the fluid conduit identified as "oxygen jets" in Figure 3. After impact with the impinging plate (Figure 3), the fluid flowed through the shear region and impacted the pintle to produce the desired hollow cone spray. The atomized liquid mixture was injected downward into the combustion zone on the central axis of the reactor to produce the flame.

The internal reactor temperatures were measured at 0.355 m intervals along the vertical axis using 3/8 in. (0.9525 cm) diameter ceramic-coated type B thermocouples. The thermocouples had a characteristic response rate of ∼5.5 °C/s for an instantaneous change from ambient to 1000 °C in air.[28] The typical accuracy of a type B thermocouple is ±4 °C at 1600 °C.[29,30] It is understood that the thermocouple readings may not represent actual gas flow temperatures/fluctuations and likely represent the local refractory temperatures and radiant environment, but are suitable to indicate relative process stability between test conditions, especially for the butanol/graphite cases. Sample Point #1 (Figure 2), located near the exit of the reactor and 1.66 m from the top of the reactor, used a nitrogen-cooled sample probe to extract flue gas samples. The combustion products left through the bottom of the reactor and entered the quench zone, in which quench water (Figure 2, Water Stream #2) was introduced via four flat fan spray nozzles located 0.3 m below the reactor outlet. The product gas was created within the quench zone but was quenched to a temperature below saturation to ensure ease of operation and to protect downstream equipment. The flue gas exited the quench vessel near the top of the vessel and entered the scrubber where the flue gas temperature was further reduced to approximately ambient temperature and exhausted. A dry gas sample was collected at Sample Point #2 (Figure 2) located near the exhaust where $O_2$ was measured using a Horiba MPA-510 gas analyzer and $CO_2$ and CO were measured using Horiba VIA-510 gas analyzers. The analyzer accuracy and characteristic response times are included in Table 5. The CO analyzer readings were corrected for excess oxygen dilution to a reference oxygen level of 3 vol % using eq 2 in order to provide a common basis of comparison between the test periods. In eq 2, 99.8 vol % is used as the oxygen purity of the oxygen mixture compared to the 20.9 vol % factor typically used for air dilution corrections. All liquid effluents were filtered through bag filters and sent for water treatment (Figure 2).


DOI: 10.1021/ef502754h
*Energy Fuels* 2015, 29, 4522−4533

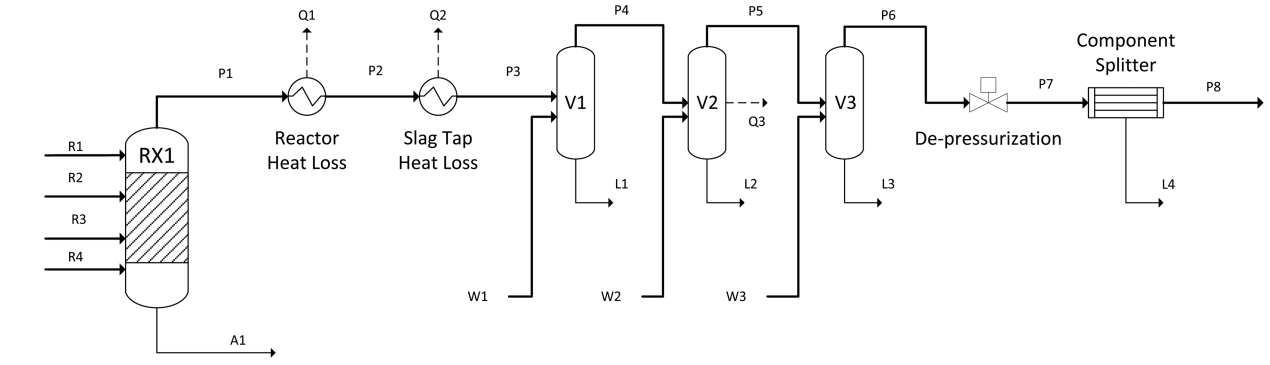


| Legend | Reactants | Products | Heat Streams | Water Streams | Liquid Streams | Unit Operations |
|---|---|---|---|---|---|---|
| R = Reactant Stream | R1 = Fuel Mixture | P1 = Flame | Q1 = Reactor Heat Loss | W1 = Water to Saturation | L1 = Saturation Condensate | RX1 = Combustor |
| P = Product Stream | R2 = Nitrogen | P2 = Combustor Outlet | Q2 = Slag Tap Heat Loss | W2 = Balance of Quench | L2 = Quench Condensate | V1 = To Saturation |
| A = Ash Stream | R3 = Oxygen | P3 = Combustion Products Wet | Q3 = Quench Heat Loss | W3 = Scrubber Water | L3 = Scrubber Condensate | V2 = Quench Outlet |
| Q = Heat Stream | R4 = Burner Moderator | P4 = Saturated Gas | | | L4 = Product Condensate | V3 = Scrubber |
| W = Water Stream | | P5 = Quench Outlet | | | | |
| L = Liquid Stream | | P6 = Scrubber Outlet | | | | |
| RX = Reactor | | P7 = Ambient Product | | | | |
| V = Vessel | | P8 = Combustion Products Dry | | | | |

**Figure 4.** Model process flow diagram for modeling of experimental results.

$$\text{corrected PPM} = \text{measured PPM} \times \frac{99.8 - 3\ \text{vol}\,\%}{99.8 - \text{O}_2\ \text{measured}} \qquad (2)$$

**2.4. Modeling of Experimental Results.** Process simulations were performed using AspenTech HYSYS. The modeling techniques used to supply the data provided in Tables 8 and 9 and Figure 6 are discussed in this section. The average feed flow and temperature values from each test period (Tables 3 and 4, B1−G1) were used as inputs. The purpose of the process simulations was to estimate the moisture content in the product gas at various intermediate stages within the process and to provide a more in-depth understanding of the pilot-plant trials. The process flow diagram of the models is shown in Figure 4.

In the model, fuel mixture (R1), nitrogen (R2), oxygen (R3, 99.8% purity), and burner moderator (R4) streams were defined using the data provided in Tables 1−4. These streams were input into a conversion reactor (RX1) in which 100% conversion was assumed. The conversion reactor outlet stream (P1) provided an estimate of the flame temperature based on the Gibbs free energy calculation performed by AspenTech HYSYS of the combustion products. The reactor heat loss (Q1) was calculated by setting the temperature of stream P2 equal to the experimentally measured combustor outlet temperatures (Tables 6 and 7).

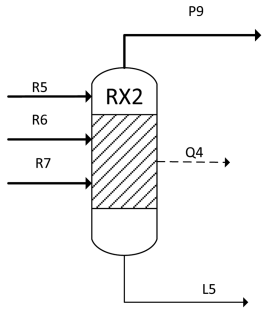


| Legend | Process Streams | Heat Streams | Unit Operations |
|---|---|---|---|
| R = Reactant Stream | R5 = Fuel Mixture | Q4 = Heat Loss | RX2 = Combustor |
| P = Product Stream | R6 = Water | | |
| L = Liquid Stream | R7 = Oxygen | | |
| Q = Heat Stream | P9 = Product | | |
| RX = Reactor | L5 = Bottoms | | |

**Figure 5.** Model process flow diagram for investigative modeling results.

Process stream Q1 represents the experimental heat loss to the refractory and surroundings as well as heat loss through the burner and sample probe cooling systems. Stream P2 was then subjected to a 3 kW heat loss (Q2) to provide the results for P3 (given as "combustion products wet" in Tables 8 and 9). Process stream Q2 represents the experimental heat loss to the slag tap and refractory support cooling. The 3 kW assumed for Q2 has been experimentally characterized based on gas temperature drops measured across the slag tap and was assumed to be constant for all the test conditions modeled.

During the pilot-plant runs, the product gas entering the quench vessel was quenched to temperatures below the steam saturation temperature (~190 °C at 1.5 MPa(g)) in order to protect back-end equipment. As a result, a large portion of the moisture was condensed out of the product gas. Therefore, in the process models, the quench vessel was separated into two vessels (V1 and V2) in order to estimate the maximum theoretically attainable $H_2O$ concentration for the given experimental conditions. For V1, the product gas stream entering the quench (P3) was quenched with just enough water (W1) to bring the outlet gas (P4) to the saturation point, such that no condensation occurred (L1 = 0). This was performed by using the adjust function to decrease the mass flow rate of W1 from the given experimental quench water flow (Tables 6 and 7) until L1 = 0. The resulting stream composition (P4) is reported as "saturated gas composition" in Tables 8 and 9. For V2, the "balance of quench" water (experimental "quench water" flow less calculated flow from W1) was input as stream W2. The experimentally measured scrubber water flow was input into V3. The resulting scrubber outlet stream (P6) was adiabatically depressurized using a valve, and the remaining water (L4) was separated using a component separator to provide the values (P8) shown as "combustion products dry" in Tables 8 and 9.

**2.5. Investigative Modeling.** Analysis of the experimental modeling results provided insight into the effects of various process parameters (fuel mixture, excess $O_2$, etc.) on the product gas $H_2O$ concentration. To further examine the effects of individual variables, investigative process modeling was performed, in which certain variables were isolated to determine their effects on the product gas. This investigative process modeling was used to produce the data presented in Figures 7 and 8. This process model (Figure 5) was a simplified process model that consisted of a conversion reactor (RX2) with fuel mixture (R5), water (R6), oxygen (R7), and heat loss (Q4) streams as inputs and a product (P9) and bottoms (L5) streams as outputs. Similar to V1, water input was adjusted until L5 was zero. Each of these streams was varied individually to produce the data trends that are plotted in Figures 7 and 8.



DOI: 10.1021/ef502754h
*Energy Fuels* 2015, 29, 4522−4533

**Table 6. Overview of Butanol Test Data**

| description | B1 | B2 | B3 | B4 |
|---|---|---|---|---|
| test run ID | 1 | 2 | 2 | 2 |
| time period (h:mm−h:mm) | 0:00−0:10 | 0:00−0:10 | 0:26−0:36 | 1:25−1:35 |
| combustor gauge pressure (kPa) | 1501.3 | 1499.6 | 1500.1 | 1499.9 |
| standard deviation of pressure (kPa) | 2.2 | 1.6 | 0.8 | 0.6 |
| combustor upper temperature (°C) | 1540 | 1510 | 1518 | 1514 |
| standard deviation of upper temperature (°C) | 2.1 | 1.7 | 1.1 | 1.7 |
| combustor outlet temperature (°C) | 1230 | 1291 | 1297 | 1427 |
| combustor heat loss (kW) | 37.1 | 36.4 | 36.3 | 27.9 |
| combustor heat loss (%) | 35.1 | 26.1 | 26.0 | 20.0 |
| quench water flow (kg/h) | 230.0 | 251.5 | 248.9 | 248.9 |
| quench outlet temperature (°C) | 125.3 | 172.5 | 178.3 | 190.5 |
| dry gas composition | | | | |
| $O_2$ (mol % dry) | 16.1 | 3.4 | 1.5 | 0.4 |
| $CO_2$ (mol % dry) | 83.6[a] | 96.3 | 98.2 | 90.6 |
| CO (ppmv dry, 3% $O_2$) | <25 | <25 | <25 | 26 |

[a]For this run, $CO_2$ concentration was determined by difference, accounting for the impurities in the oxidant through a mass balance.

**Table 7. Graphite and Mixture Test Results Summary**

| description | BG1 | BG2 | BG3 | BG4 | G1 | G2 |
|---|---|---|---|---|---|---|
| time period (h:mm−h:mm) | 0:03−0:09 | 0:10−0:19 | 0:19−0:23 | 0:50−0:56 | 0:57−1:03 | 1:09−1:11 |
| combustor gauge pressure (kPa) | 1499.9 | 1499.4 | 1502.0 | 1501.6 | 1501.4 | |
| standard deviation of pressure (kPa) | 2.2 | 1.9 | 2.1 | 4.2 | 11.5 | |
| combustor upper temperature (°C) | 1527 | 1588 | 1555 | 1568 | 1602 | 1605 |
| standard deviation of upper temperature (°C) | 2.7 | 3.0 | 4.6 | | 17.6 | |
| combustor outlet temperature (°C) | 1333 | 1388 | 1370 | 1350 | 1331 | 1341 |
| combustor heat loss (kW) | 53.3 | 52.2 | 53.7 | 53.3 | 62.2 | 62.6 |
| combustor heat loss (%) | 30.3 | 29.2 | 30.1 | 37.8 | 49.3 | 38.1 |
| quench water flow (kg/h) | 262.8 | 267.5 | 262.8 | 291.5 | 289.7 | 287.5 |
| quench outlet temperature (°C) | 161.3 | 160.3 | 158.9 | 145.5 | 128.2 | 132.5 |
| dry gas composition | | | | | | |
| $O_2$ (mol % dry) | 5.9 | 6.0 | 0.4 | 4.0−15.5 | 20.7−27.6[a] | 2.5−7.9 |
| $CO_2$ (mol % dry) | 93.7 | 93.5 | 99.3 | 95.8−84.3 | 79.1−72.2 | 92.0−97.4[a] |
| CO (ppmv dry, 3% $O_2$) | <25 | <25 | <25−1644 | 650−1225 | 205−465 | 100−335 |

[a]Determined by difference with a check from the mass balance.

## 3. RESULTS

**3.1. Experimental Results of Butanol Tests.** The four *n*-butanol test periods took place over two separate runs. Butanol test period 1 (B1) data are shown to span from 0:00 to 0:10 (h:mm) of the first run. Butanol test periods 2 (B2) and 3 (B3) data were selected to, respectively, span from time 0:00 to 0:10 and 0:26 to 0:36 of the second test run. Butanol test period 4 (B4) data spanned from 1:25 to 1:35 of the second test run. A summary of the test data for test periods B1−B4 is presented in Table 6.

For B1, the $O_2$ concentration was 16 mol % on a dry basis. The $O_2$ level was set high because the objective of this test period was to serve as a proof-of-concept in which very safe operating conditions were selected. Over this test period, CO was below detection limits (<25 ppmv dry, 3% $O_2$), indicating excellent conversion to $CO_2$. For B2, the $O_2$ concentration was much lower at 3.4 mol % on a dry basis. This was the first test in which attempts to run at low $O_2$ concentration were made. The CO content was again below detection limits (<25 ppmv dry, 3% $O_2$), which indicates significant flame stability and conversion to $CO_2$. The $O_2$ concentration throughout B3 was around 1.52 mol % on a dry basis. The lowest $O_2$ content was achieved during test period B4, in which it was about 0.4 mol % on a dry basis. The CO fluctuated at around 26 ppmv (dry, 3% $O_2$), which indicates that the conversion of CO to $CO_2$ was still very high. For both runs, the upper reactor temperature and reactor pressure were very stable (Table 6) with standard deviations of no greater than 2.1 °C and 2.2 kPa, respectively, indicating low reaction and gross flow field fluctuations. These low deviations, coupled with the low CO emissions (less than 50 ppmv dry, 3% $O_2$), indicate that the flame was very stable and that the conversion to $CO_2$ was very high.

**3.2. Experimental Results for Graphite and Butanol/Graphite Mixtures.** The nature of the testing and the difficulty in combusting graphite resulted in greater fluctuations in temperature and gas compositions compared to the results from *n*-butanol tests B1−B4. Furthermore, feeding issues with the graphite−water slurry caused by graphite settling and plugging of the feed lines resulted in the need for sudden and dramatic operating changes in the reactant flows. As a result, the test period time spans were shorter, more transient, and of varying lengths compared to the simpler operation of the butanol tests. Although the test periods are outlined to span a certain time frame, the experimental results in Table 7 are presented as a range in numbers to provide qualitative observations and do not necessarily represent steady-state operation. The time frames for


DOI: 10.1021/ef502754h
*Energy Fuels* 2015, 29, 4522−4533

**Table 8. Modeling Results Summary for *n*-Butanol Runs**

| description | B1 | B2 | B3 | B4 |
|---|---|---|---|---|
| flame temperature (°C) | 1939 | 1802 | 1807 | 1809 |
| combustion products composition dry | | | | |
| $O_2$ (mol % dry) | 16.1 | 3.3 | 1.5 | 0.4 |
| $CO_2$ (mol % dry) | 83.6 | 96.4 | 98.2 | 93.6 |
| $N_2$ (ppmv dry, 3% $O_2$) | 592 | 598 | 595 | 5.75[a] |
| Ar (ppmv dry, 3% $O_2$) | 2367 | 2393 | 2379 | 2319 |
| combustion products composition wet | | | | |
| $H_2O$ (mol % wet) | 77.8 | 81.7 | 82.0 | 81.3 |
| $O_2$ (mol % wet) | 3.57 | 0.60 | 0.27 | 0.08 |
| $CO_2$ (mol % wet) | 18.6 | 17.7 | 17.7 | 17.5 |
| $N_2$ (ppmv wet, 3% $O_2$) | 131 | 110 | 107 | 10729 |
| Ar (ppmv wet, 3% $O_2$) | 526 | 439 | 429 | 433 |
| CO (ppmv wet, 3% $O_2$) | 3 | 2 | | 5 |
| water to saturation | 50.8 | 77.9 | 78.3 | 89.0 |
| saturation temperature | 195.1 | 196.3 | 196.9 | 197.1 |
| saturated gas composition | | | | |
| $H_2O$ (mol % wet) | 88.0 | 90.5 | 90.7 | 91.0 |
| $O_2$ (mol % wet) | 1.93 | 0.32 | 0.14 | 0.04 |
| $CO_2$ (mol % wet) | 10.0 | 9.2 | 9.1 | 8.5 |
| $N_2$ (ppmv wet, 3% $O_2$) | 15 | 57 | 55 | 5186 |
| Ar (ppmv wet, 3% $O_2$) | 284 | 227 | 222 | 209 |
| CO (ppmv wet, 3% $O_2$) | 2 | 1 | | 2 |
| balance of quench (kg/h) | 179.2 | 173.6 | 170.6 | 159.9 |

[a]Unit is mol % dry as a result of extra $N_2$.

the test periods are mostly meant to bound general operating states in order to provide average reactant inlet feed compositions to be used for the modeling portion of this work. Modeling was used to provide quantitative insight into the results that would be theoretically expected if the reactor were operating at steady state under those conditions.

All of the butanol/graphite test periods took place over one run. Butanol/graphite test period 1 (BG1) spanned from time 0:03 to 0:09 (h:mm) after steady operation was achieved. Butanol/graphite test period 2 (BG2) spanned from time 0:10 to 0:19. For butanol/graphite test period 3 (BG3), which spanned from 0:19 to 0:23, the oxygen flow was reduced to around 50 kg/h and the water moderator to the burner was reduced to 38 kg/h for a total of 55.3 kg/h water (including water in the slurry). The CO content increased throughout this period due to a combination of fuel feed flow instabilities caused by the graphite−water slurry and the stoichiometry dropping closer to 1. Butanol/graphite test period 4 (BG4) spanned from time 0:50 to 0:56, in which the butanol flow rate was reduced to increase the graphite fraction in the fuel mixture. The average flows over the time period were used for the simulation in order to model this low *n*-butanol test condition. After BG4, the butanol flow to the burner was stopped, the burner water moderator was decreased to about 6 kg/h, and the slurry flow rate was slowly increased. Graphite test period 1 (G1) spanned from time 0:57 to 1:03 with the slurry flow rate increasing from 30 to 34 kg/h over that time and the dry molar $O_2$ content reaching a point where it exceeded the range of the $O_2$ analyzer (approximately 24 mol %). The $O_2$ content in the flue gas for this time period was thus determined by assuming that $CO_2$ was the balance of the dry gas with a check based on a mass balance of the flows entering the reactor. Following G1, the water moderator flow was increased to 20 kg/h and the $O_2$ flow was reduced to 45 kg/h. Graphite test period 2 (G2) took place at these conditions from time 1:09 to 1:11. Throughout that period, the $CO_2$ analyzers began to fluctuate and, due to the short time frame, never reached a stable reading. The $CO_2$ concentration was back-calculated from the $O_2$ readings and do not reflect the analyzer measurements. A check on the back calculation was performed via stoichiometric calculations from the feed flows. The graphite test period data were difficult to analyze because there were issues with temporary burner plugging due to settling of particles, in the slurry line. The upper reactor temperature fluctuations indicate that the process was unstable for graphite only combustion. Overall, unassisted combustion of graphite−water slurry was achieved for a period of 20 min. BG3 and BG4 indicate that it is possible to sustain a flame using low-volatile fuels in this pressurized oxy-fuel combustion direct contact steam generation firing mode, but the flame was not as easily sustained for G1 and G2. Feeding issues with the slurry will need to be addressed.

Over the butanol/graphite test periods, the CO emissions ranged from less than 25 ppmv to about 1225 ppmv (dry, 3% $O_2$), which corresponds to a maximum of 240 ppmv in the wet product gas. Although CO fluctuated significantly, it seemed to generally increase when the graphite content of the fuel mixture was increased and/or when the $O_2$ flow to the burner was decreased below a threshold that was close to the stoichiometric point. Periods where the stoichiometry was below 1 are not included in the analysis because the CO analyzer readings were not spanned for CO above 2500 ppmv and substoichiometric conditions were not part of the test plan. Future work with analyzers calibrated for a higher range will include substoichiometric combustion conditions. The periods of relatively low CO emissions (such as BG1 and BG2) indicate that good conversion of carbon is achievable, especially considering the low $O_2$ content in the wet gas (around 1.6 mol % in the combustor for BG1 and BG2). For the higher butanol mixture in BG1−BG3, very little fluctuation in the combustor upper temperature and reactor pressure was observed (with standard deviation ranging from 2.7 to 4.6 °C and 1.9 to 2.1 kPa, respectively), indicating that the


DOI: 10.1021/ef502754h
*Energy Fuels* 2015, 29, 4522−4533

Table 9. Modeling Results Summary for *n*-Butanol/Graphite Runs

| description | BG1 | BG2 | BG3 | BG4 | G1 |
|---|---|---|---|---|---|
| flame temperature (°C) | 1959 | 1989 | 1994 | 2134 | 2393 |
| combustion products composition dry | | | | | |
| $O_2$ (mol % dry) | 5.9 | 6.0 | 0.4 | 22.9[a,b] | 27.1[a] |
| $CO_2$ (mol % dry) | 93.8 | 93.7 | 99.4 | 76.9 | 72.8 |
| $N_2$ (ppmv dry, 3% $O_2$) | 464 | 461 | 462 | 429 | 900 |
| Ar (ppmv dry, 3% $O_2$) | 1856 | 1845 | 1847 | 1717 | 1804 |
| combustion products composition wet | | | | | |
| $H_2O$ (mol % wet) | 72.9 | 72.5 | 73.0 | 61.3 | 46.6 |
| $O_2$ (mol % wet) | 1.60 | 1.66 | 0.11 | 8.84 | 14.5 |
| $CO_2$ (mol % wet) | 25.4 | 25.8 | 26.8 | 29.7 | 38.8 |
| $N_2$ (ppmv wet, 3% $O_2$) | 125 | 127 | 124 | 166 | 410 |
| Ar (ppmv wet, 3% $O_2$) | 502 | 507 | 498 | 664 | 822 |
| CO (ppmv wet, 3% $O_2$) | 3 | 3 | 3−433 | 251−474 | 87−198 |
| water to saturation | 94.4 | 99.1 | 97.5 | 70.3 | 52.55 |
| saturation temperature | 194.4 | 199.4 | 194.4 | 190.9 | 186.5 |
| saturated gas composition | | | | | |
| $H_2O$ (mol % wet) | 86.5 | 86.6 | 86.8 | 80.8 | 73.2 |
| $O_2$ (mol % wet) | 0.80 | 0.81 | 0.06 | 4.40 | 7.3 |
| $CO_2$ (mol % wet) | 12.7 | 12.5 | 13.1 | 14.8 | 19.5 |
| $N_2$ (ppmv wet, 3% $O_2$) | 62 | 73 | 61 | 83 | 190 |
| Ar (ppmv wet, 3% $O_2$) | 250 | 293 | 243 | 332 | 380 |
| CO (ppmv wet, 3% $O_2$) | 2 | 2 | | | |
| balance of quench (kg/h) | 168.4 | 168.4 | 165.3 | 221.2 | 237.1 |

[a]Based on the average flows over the test period. [b]Does not correlate to analyzers due to response lag to step change in *n*-butanol flow.

flame was stable for this mixture. The flame stability decreased for the lower butanol-containing mixture in BG4 (standard deviation of 4.2 kPa) and was worse for G1 (standard deviation of 17.6 °C and 11.5 kPa) and not measurable for G2. There was no measurable carbon-containing residues found in the liquid and gas bag filters, indicating that no unburned carbon made it through the system, and thus high solids conversion was achieved, regardless of the lower operating stabilities experienced.

**3.3. Modeling Results.** The modeling results for the butanol runs are presented in Table 8. The modeling results for graphite−water slurry and butanol/graphite−water slurry mixtures are shown in Table 9. The CO values given in Table 8 and Table 9 were incorporated into the results from the analyzer readings given for the respective test period, corrected for $H_2O$ dilution to a reference of 3 vol % $O_2$. The CO correction is given in eq 3.

$$CO_{wet} = CO_{dry(3\%\ O_2)} \times \frac{100 - H_2O_{concentration}}{100} \quad (3)$$

It was not possible to provide an accurate comparison between the modeling and experimental results of graphite combustion under different firing scenarios because there was not enough reliable data produced; therefore, the models assumed the average reactant flows observed in G1. Process modeling for G2 was not performed as the experimental data were too unreliable.

## 4. DISCUSSION

For B1, the maximum attainable steam content was calculated to be 88 mol %, whereas it was calculated to be approximately 90.5 mol % for B2. This was attributed to the significantly lower $O_2$ content in the flue gas in the B2 test. The $O_2$ content may affect the maximum attainable steam concentration because its increased partial pressure will lower the saturation temperature of the mixture since $O_2$ is noncondensable in these conditions. The maximum attainable steam concentration calculated for B3 was 90.7 mol %. For B4, the lowest $O_2$ content had the highest maximum attainable steam concentration (91.0 mol %). Although the data support the hypothesis that $O_2$ concentration will have an effect on the maximum attainable steam concentration, the difference is within experimental error limits, making this effect difficult to quantify without further investigation. The maximum steam concentration achieved for the graphite tests was around 80.5 mol % on average. For tests BG1−BG3, it was around 86.5 mol %, and for BG4, it was around 81 mol %.

In all of the *n*-butanol cases (B1−B4), CO production was minimal. This indicates that the fuel was being fully converted in all cases. This result opens up the possibility of operating the combustor slightly substoichiometrically with the goal of producing a product gas with oxygen concentrations less than 100 ppmv (dry). This process is ideal for a low-$O_2$ operating condition because the combustion products are being further diluted with water downstream. For example, if combustion results in a 1 mol % $O_2$ concentration in the dry gas, it will be diluted to as low as around 0.1 mol % in a 90 mol % steam product gas.

When the standard deviations (Table 6) on the upper reactor temperature and reactor pressure were calculated for B1−B4, it was observed that the deviations were no larger than 2.1 °C and 2.2 kPa for temperature and pressure, respectively. These numbers indicate low fluctuations in the conversion (temperature) and stable flow fields (pressure) within the reactor. These results, coupled with the low CO emissions, indicate that the flame was quite stable throughout the testing. This observed process stability for the high-volatile fuel shows that combustion is not significantly impeded by the high concentration of steam and the flame quenching imposed by the vaporization of the water. This was not the case for the graphite combustion. When the graphite−water slurry was added (BG1−G2), low CO


DOI: 10.1021/ef502754h
Energy Fuels 2015, 29, 4522−4533

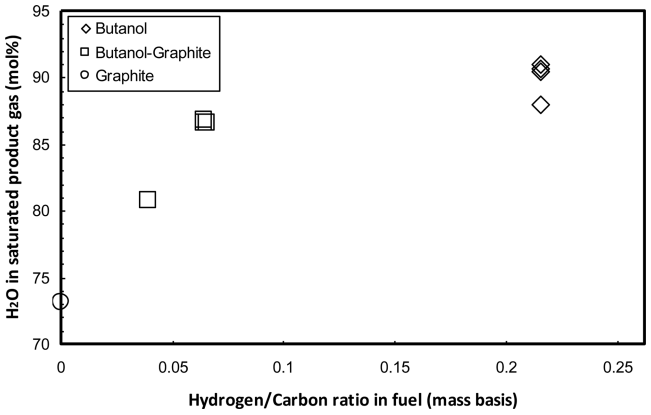


**Figure 6.** Maximum attainable steam concentration (effect of fuel H/C ratio).

emissions were only achievable with high amounts of excess $O_2$ and the process stability decreased with increasing graphite addition as a result of fuel feed variability. Apart from reducing fuel feed variability, a method that has been suggested to improve process stability is the Moderate or Intense Low-oxygen Dilution (MILD) combustion condition.[31,32] MILD combustion is a flameless oxidation process, in which the reactants are preheated to high temperatures and entrained with high-temperature exhaust gases to dilute the fuel and oxidant jets.[33] The main advantages of MILD combustion are uniform temperature distribution, increased net radiation flux, extremely low $NO_x$ emissions, and stable operation without flame stabilization problems.[31] At present, it appears that little work has been done using MILD combustion with a superheated steam exhaust gas recycle. Furthermore, recycle schemes for high-temperature DCSG products have not been investigated. For these reasons, the DCSG process has not been operated using the MILD combustion condition, but this may be a subject of future work.

Overall, low $O_2$ contents were attainable during HiPrOx/DCSG combustion of the volatile fuel (as low as 0.08 mol % dry) without significant CO production. Furthermore, the increased addition of $H_2O$ to attain the product gas composition results in an $O_2$ content as low as 0.04 mol % wet, or 4000 ppmv wet. Field tests performed by Yee and Stroich,[23] in which they injected a flue gas generated by a fuel-rich natural gas-fired internal combustion engine into a SAGD well, found that, after four months of operation, none of the carbon steel corrosion monitoring devices showed signs for concern. The flue gas composition for these field tests was 100 ppmv $O_2$, 16.15 mol % $CO_2$, 81.5 mol % $N_2$, 1.34 mol % $H_2$, and 0.71 mol % CO (all on a dry basis). Although the excess $O_2$ for the tests performed in this study was higher than that of Yee and Stroich, future work will investigate operation that is slightly substoichiometric with the objective of minimizing $O_2$ in the flue gas and, thus, potential corrosion issues.

As previously mentioned, the $H_2O$ content in the product gas is important because of the latent heat that it contributes as it condenses in the bitumen reservoir. The test results indicate that a $H_2O$ content in the product gas of around 90 mol % is attainable at the saturation point using *n*-butanol at the pilot scale. Although this is favorable from an energy efficiency standpoint, heat losses in transport pipes may cause condensation and corrosion due to the formation of carbonic acid. Yee and Stroich[23] suggested that, if the flue gas is always above its dew point, the potential for corrosion from carbonic acid would be reduced. One method of ensuring this with the HiPrOx/DCSG technology would be to operate the scrubber at a vapor phase fraction of around 0.9 to avoid scaling issues and then to superheat the scrubber outlet gas to a temperature above the acid dew point. This will result in $H_2O$ contents in the product gas that are below 90 mol % wet but also well above 80 mol % wet, which was the $H_2O$ content in the combustion products at 1800 °C (Table 8). This leaves 1400 °C of heat in the flue gas that can be quenched through the addition of water. A sensitivity analysis regarding the effect of the product gas outlet temperature on the water and fuel requirements per barrel of oil produced will be considered in future work to determine the optimal operating conditions.

Figure 6 compares the experimental fuel hydrogen-to-carbon ratio (H/C ratio, mass basis) with the theoretical maximum attainable $H_2O$ concentration in the product gas. It can be observed that $H_2O$ content in the flue gas increases with an increasing ratio of hydrogen to carbon in the fuel. This is expected because the saturation point of the gas is affected by the partial pressure of the balance noncondensable combustion products (mainly $CO_2$). Therefore, a fuel that produces more water as a combustion product compared to $CO_2$ will produce a product gas with a higher purity steam. This occurs because the partial pressure of $CO_2$ will be further lowered after additional water has been injected downstream to further cool the flue gas and produce more steam. The experimental data support this conclusion. The graphite−water slurry tests show that the steam purity achieved was around 80.5 mol % on average. For tests BG1−BG3, it was around 86.5 mol %, and for BG4, it was around 81 mol %. The butanol tests gave a steam purity of 90 mol %. When the maximum steam concentration results are compared with the H/C ratio of the fuels given in Tables 1 and 2, it can be observed that the highest steam production favors fuels with high H/C ratios such as natural gas. This indicates that a high H/C ratio fuel such as natural gas would produce an even higher purity steam product. In summary, care must be taken when selecting the fuel for a DCSG process because the fuel will have an effect on the product gas, with fuels containing higher H/C ratios resulting in the highest $H_2O$ purity and thus the greatest steam generating efficiency.

Further examination using process modeling found that excess $O_2$ also plays a role on the outlet saturation concentration because it affects the composition of the balance gas after the additional water has been added. The higher the $O_2$ concentration in the product gas, the lower the $H_2O$ concentration in the saturated flue gas because of the effect that $O_2$ has on the balance gas. Figure 7 illustrates the effect of excess $O_2$ concentrations on the maximum attainable steam concentration for various fuel H/C ratios. It can be seen that increased $O_2$ in the flue gas (i.e., increased excess $O_2$) results in decreased $H_2O$ concentration over the entire range of fuel H/C ratio. This results from dilution by the noncondensable gas. In summary, it is important to reduce excess $O_2$ when designing a DCSG process in order to maximize the $H_2O$ purity in the product gas.

Process modeling of the pilot plant data also revealed the effect that heat loss has on the product gas purity. This was observed when experimental results deviated from the theoretical prediction of maximum attainable steam concentration. The effect of heat loss was further investigated using process modeling to calculate the maximum steam concentration for various heat loss fractions over a range of fuel H/C ratios. The results are illustrated in Figure 8. From the curves, it can be seen


DOI: 10.1021/ef502754h
*Energy Fuels* 2015, 29, 4522−4533

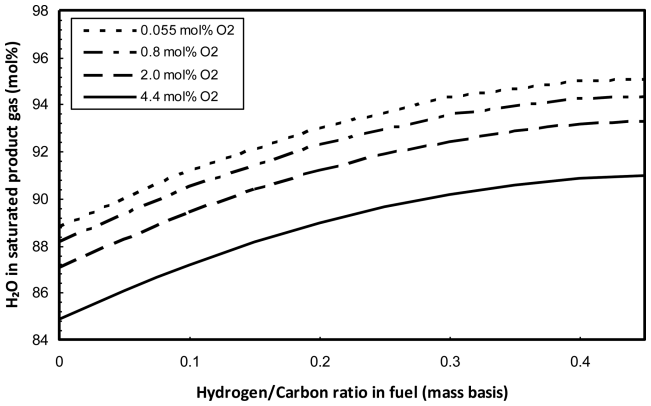


**Figure 7.** Maximum attainable steam concentration (effect of fuel H/C ratio) with various $O_2$ concentrations in the product gas.

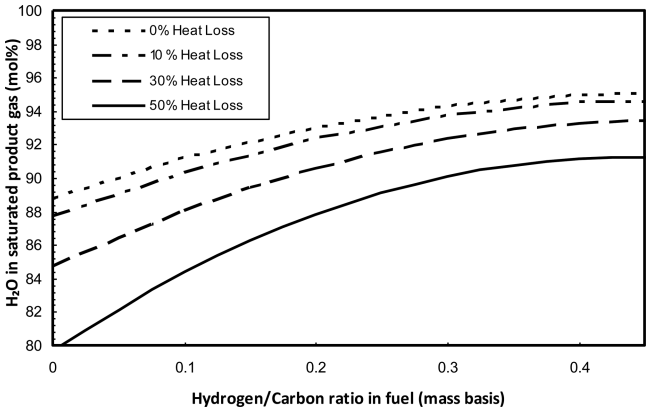


**Figure 8.** Maximum attainable steam concentration (effect of fuel H/C ratio) with various heat losses to the system.

that any heat losses to the system will affect the outlet conditions. Mainly, any heat lost from the system is heat that is unused to evaporate $H_2O$, which reduces the maximum attainable $H_2O$ content in the product gas.

Another interesting trend observed in Figure 8 is the combined effect of the fuel H/C ratio and heat loss. The diverging curves with decreasing H/C ratio indicate that the lower the H/C ratio of the fuel, the greater the effect of heat loss. Fuels with lower H/C ratios require more addition of water to reach the saturation point than fuels with higher H/C ratios because less $H_2O$ is produced through chemical reaction of the fuel. Therefore, for the lower H/C ratio fuels, a greater amount of the total steam produced has to come from heat to the feedwater rather than conversion of the fuel to steam directly, making these fuels more dependent on heat from combustion and thus more sensitive to heat loss.

## 5. CONCLUSION

Proof-of-concept pilot-plant testing and process modeling of the HiPrOx/DCSG process were performed in this study. Pilot-plant testing indicated that, for the butanol test periods (B1−B4), the process was very stable and the CO emissions (<25 ppmv dry, 3% $O_2$) were below detection limits. These results indicate that very stable process operation with highly volatile fuels is possible with the large amounts of water quenching required for the DCSG process. For the mixtures containing higher butanol-to-graphite ratios (BG1 and BG2), low CO emissions (<25 ppmv dry, 3% $O_2$) were achieved with relatively stable operation. As the fraction of graphite−water slurry was increased (BG3−G2), the process stability decreased and the CO emissions increased, even for cases with high excess oxygen. Fuel feed delivery issues with the graphite−water slurry may have been the contributing factor to the instabilities. These results outline the difficulties of feeding slurried solids in a manner that will lead to stable operation. In the future, existing combustion and gasification technologies that successfully feed coal and petroleum coke slurries into pressurized reactors can be used as a reference to improve performance.

It was observed via process modeling that the fuel H/C ratio, excess $O_2$, and heat loss are important parameters when considering a DCSG system because they directly affect the process performance and quality of the desired product. The process modeling indicated that fuels with high H/C ratios are more favorable because they yield greater $H_2O$ concentrations in the product gas; heat loss must be minimized, especially for fuels with low H/C ratios because they are more dependent on the heat of combustion to produce steam; and the presence of noncondensable gases ($O_2$, $N_2$) should be minimized in order to avoid dilution of the product gas.

In conclusion, pilot-plant testing indicates that stable combustion of a volatile fuel such as *n*-butanol is easily achievable for this high-moisture DCSG process. Mixtures of butanol and graphite−water slurry also resulted in stable operation, but combustion of pure graphite−water slurry was difficult due to feed variability issues. These trials serve as a proof-of-concept of this novel technology and indicate that further investigation is warranted. Process modeling indicates that fuels with high H/C ratios are more favorable. Also, heat loss, excess $O_2$, and the presence of other noncondensable gases should be minimized to generate a higher purity steam product. This differs from conventional combustion systems in which the flue gas is most commonly used as a source of heat rather than as part of the product.

## ■ ASSOCIATED CONTENT

### Supporting Information

Test period data trends. The Supporting Information is available free of charge on the ACS Publications website at DOI: 10.1021/ef502754h.

## ■ AUTHOR INFORMATION

### Corresponding Author

*Tel: 613-943-1688. E-mail: paul.cairns@nrcan.gc.ca.

### Author Contributions

The manuscript was written through contributions of all authors. All authors have given approval to the final version of the manuscript.

### Notes

The authors declare no competing financial interest.

## ■ ACKNOWLEDGMENTS

The authors would like to acknowledge that funding for this work was provided by Natural Resources Canada through the Program of Energy Research and Development and by the Natural Sciences and Engineering Research Council (NSERC) of Canada. We would also like to acknowledge Jeff Slater and Ryan Burchat for technical assistance in operating the pilot-scale facility. The authors would also like to acknowledge Brandon Lowe for his help in finalizing this paper.



DOI: 10.1021/ef502754h
*Energy Fuels* 2015, 29, 4522−4533

## ABBREVIATIONS

SAGD=steam-assisted gravity drainage
HiPrOx/DCSG=high-pressure oxy-fired direct contact steam generation
CCS=carbon capture and storage

## REFERENCES


(1) *Alberta Oil Sands Industry Quarterly Update: Winter 2015* (reporting on the period: Sep 27, 2014 to Dec 04, 2014); JuneWarren-Nickle's Energy Group: Calgary, Alberta, Canada, 2014; p 2.
(2) *In-situ Process Steam Assisted Gravity Drainage*; Alberta Government: Edmonton, Alberta, Canada, 2013; p 1.
(3) Bohm, M.; Goold, S.; Laux, S.; Neu, B.; Sharma, A.; Aasen, K. *Energy Procedia* **2011**, *4*, 958−965.
(4) Clements, B. (Her Majesty the Queen in Right of Canada as Represented by the Minister of Natural Resources, assignee) High pressure direct contact oxy-fired steam generator. United States patent US 20110232545A1, Aug 29, 2011.
(5) Gates, I. D.; Bunio, G.; Wang, J.; Robinson, B. Impact of Carbon Dioxide Co-injection on the Performance of SAGD. In *Proceedings of the 2011 World Heavy Oil Congress*, Edmonton, Alberta, Canada, March 14−17, 2011.
(6) Cairns, P. E. High Pressure Oxy-fired (HiPrOx) Direct Contact Steam Generation (DCSG) for Steam Assisted Gravity Drainage (SAGD) Application. Master's Thesis, University of Ottawa, Ottawa, ON, Canada, 2013, pp 11−40.
(7) Sarkar, S. *J. Inst. Eng. (India), Chem. Eng. Div.* **1988**, *68*, 55−58.
(8) Alamatsaz, A.; Moore, R.; Mehta, S.; Ursenbach. *J. Can. Pet. Technol.* **2011**, *50*, 48−67.
(9) Mohtadi, M.; Sarkar, S. *Can. J. Chem. Eng.* **1985**, *63*, 674−680.
(10) Betzer-Tsilevich, M. Integrated Steam Generation Process and System for Enhanced Oil Recovery. In *Proceedings of the 2010 Canadian Unconventional Resources & International Petroleum Conference*, Calgary, Alberta, Canada, Oct 19−21, 2010.
(11) Sadhukan, A.; Gupta, P.; Saha, R. *Fuel* **2010**, *89*, 162−169.
(12) Goard, P.; Mulcahy, M. *Carbon* **1967**, *5*, 137−153.
(13) Sun, C.; Zhang, M. *Combust. Flame* **1998**, *115*, 267−274.
(14) Toftegaard, M.; Brix, J.; Jensen, P.; Glarborg, P.; Jensen, A. *Prog. Energy Combust. Sci.* **2010**, *36*, 1−45.
(15) Hu, Y.; Nikzat, H.; Nawata, M.; Kobayashi, N.; Hasatani, M. *Fuel* **2010**, *80*, 2111−2116.
(16) Wang, C.; Lei, M.; Yan, W.; Wang, S.; Jia, L. *Energy Fuels* **2011**, *25*, 4333−4344.
(17) Yu, J.; Harris, D.; Lucas, J.; Roberts, D.; Wu, H.; Wall, T. *Energy Fuels* **2004**, *18*, 1346−1353.
(18) Monson, C.; Germane, G.; Blackham, A.; Smoot, D. *Combust. Flame* **1994**, *100*, 669−683.
(19) Yang, T.; Balles, E.; Lisauskas, R.; Vitalis, B.; Hunt, P. Pressurized Oxycombustion Carbon Capture Power System. In *Proceedings of the 35th International Technical Conference on Clean Coal & Fuel Systems*, Clearwater, Florida, USA, June 6−10, 2010.
(20) Wall, T.; Lui, G.; Wu, H.; Roberts, D.; Benfell, K.; Gupta, S.; et al. *Prog. Energy Combust. Sci.* **2002**, *28*, 405−433.
(21) Riaza, J.; Álvarez, L.; Gil, M.; Pevida, C.; Pis, J.; Rubiera, F. *Energy* **2011**, *36*, 5314−5319.
(22) Seepana, S.; Jayanti, S. *Energy Convers. Manage.* **2010**, *51*, 1981−1988.
(23) Yee, C. T.; Stroich, A. *J. Can. Pet. Technol.* **2004**, *43*, 54−61.
(24) Makino, A.; Fujizaki, H.; Araki, N. *Combust. Flame* **1998**, *113*, 258−263.
(25) Culbertson, B.; Brezinsky, K. *Proc. Combust. Inst.* **2011**, *33*, 1837−1842.
(26) Lang, T.; Hurt, R. H. *Proc. Combust. Inst.* **2002**, *29*, 423−431.
(27) *TIMCAL TIMREX KS5-75TT Graphite Data Sheet: Primary Synthetic Graphite*, V09; MatWeb: Blacksburg, VA, 2014.
(28) Correspondence: Tim Forman, SynTemp Thermocouples, March, 2015.
(29) *Thermocouple Accuracies*; Reotemp Instruments: San Diego, CA. http://reotemp.com/thermocoupleinfo/thermocouple-accuracies.htm (accessed: March 2015).
(30) *Technical Notes: Thermocouple Accuracy*; Microlink Engineering Solutions: Manchester, U.K. http://www.microlink.co.uk/tctable.html (accessed: March 2015).
(31) Li, P.; Wang, F.; Mi, J.; Dally, B. B.; Mei, Z. *Energy Fuels* **2014**, *28* (2), 1524−1535.
(32) Li, P.; Dally, B. B.; Mi, J.; Wang, A. *Combust. Flame* **2013**, *160* (5), 933−946.
(33) Noor, M. M.; Wandel, A. P.; Yusaf, T. *Int. J. Automot. Mech. Eng.* **2012**, *6*, 730−754.



DOI: 10.1021/ef502754h
*Energy Fuels* 2015, 29, 4522−4533